Supplementary Information

Room temperature synthesis of thiostannates applying the novel compound $\{[Ni(tren)]_2[Sn_2S_6]\}_n$ as precursor

Jessica Hilbert, Christian Näther, Richard Weihrich, Wolfgang Bensch*

Content

Table S1: Selected details of the data collection and results of the structure refinements

	1	2	3
crystal system	monoclinic	monoclinic	monoclinic
space group	*C*2/*c*	$P2_1/n$	$P2_1/n$
M (g/ mol)	839.64	1009.86	1023.94
a (Å)	23.371(3)	11.1715(3)	12.9264(3)
b (Å)	8.231(2)	10.5384(3)	10.1627(3)
c (Å)	14.274(2)	15.8594(5)	15.6585(4)
α (°)	90	90	90
β (°)	107.230(10)	101.833(2)	113.263(2)
γ (°)	90	90	90
V ($Å^3$)	2622.6(8)	1827.45(9)	1889.78(9)
temperature (K)	293(2)	200(2)	200(2)
Z	4	2	2
$D_{calculated}$ (g/ cm^3)	2.127	1.835	1.799
μ (mm^{-1})	3.79	2.751	2.656
scan range (deg)	$4 \leq \theta \leq 54$	$2.05 \leq \theta \leq 27.93$	$1.74 \leq \theta \leq 27.005$
reflections collected	3441	28097	26578
independent reflections	2868	4371	4120
observed reflections	2044	3760	3712
goodness-of-fit on F^2	1.003	1.022	1.067
R values ($I > 2\sigma(I)$)	R1 = 0.0340	R1 = 0.0261,	R1 = 0.0239
	wR2 = 0.0838	wR2 = 0.0637	wR2 = 0.0575
R values (all data)	R1 = 0.0710	R1 = 0.0339,	R1 = 0.0288
	wR2 = 0.0933	wR2 = 0.0656	wR2 = 0.0590
res. elec. dens. (e/$Å^3$)	1.28/-0.76	0.788/-0.560	0.511/-0.780

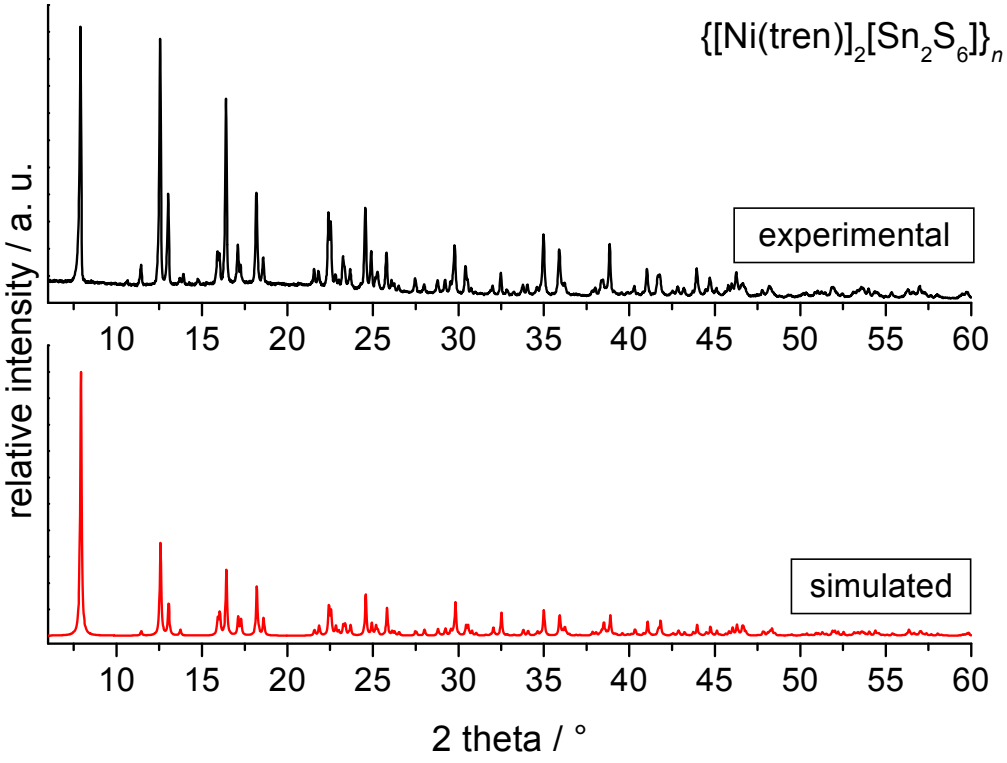
{[Ni(tren)]2[Sn2S6]}n
relative intensity / a. u.
experimental
simulated
10 15 20 25 30 35 40 45 50 55 60
2 theta / °

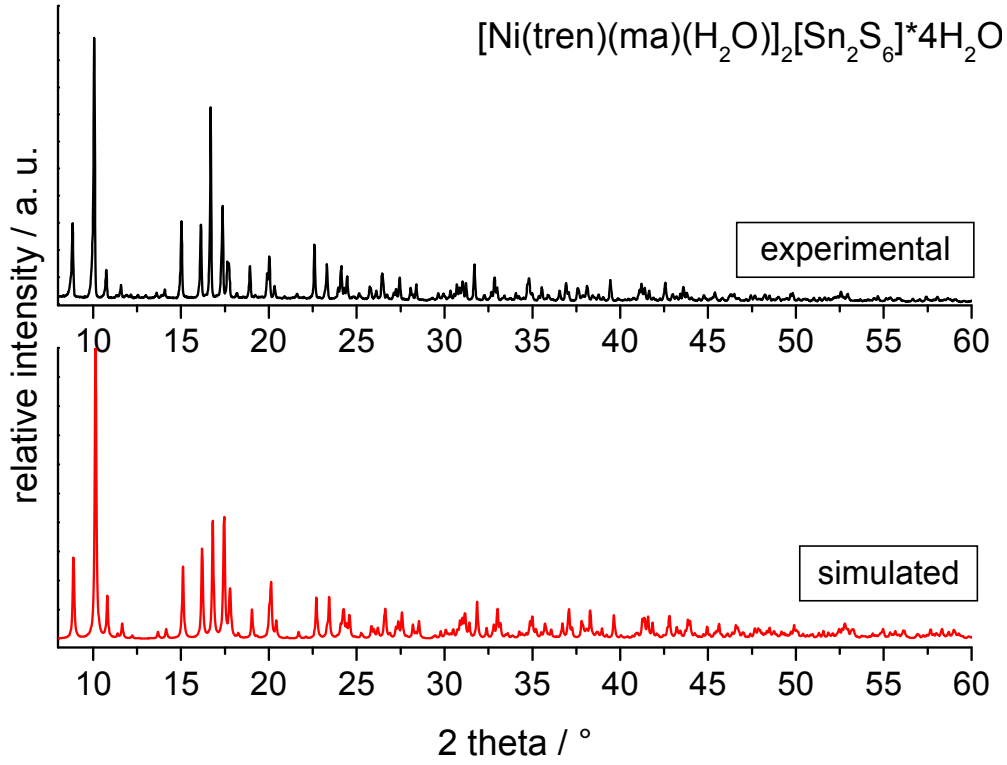
[Ni(tren)(ma)(H2O)]2[Sn2S6]*4H2O
relative intensity / a. u.
experimental
simulated
10 15 20 25 30 35 40 45 50 55 60
2 theta / °

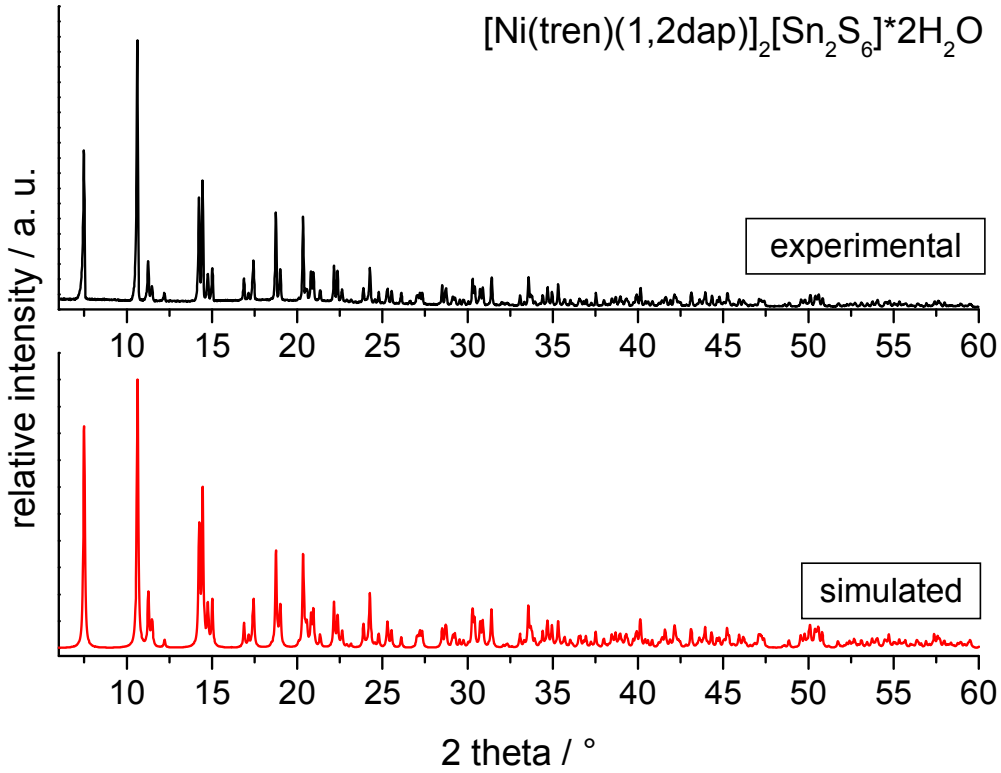

Fig. S1: Comparison of the experimental PXRD patterns of **1-3** (black) with their corresponding simulated from single-crystal X-ray data (red).

The lattice parameters for compound $[Ni(tren)(1,2\text{-}dap)]_2[Sn_2S_6] \cdot 2H_2O$ at room temperature were determinate from the PXRD pattern (Table S1). For this compounds these lattice parameters were used for the simulated patterns. For the two other compounds, no major deviation could be observed.

Table S2: Comparison of the lattice parameters for compound $[Ni(tren)(1,2\text{-}dap)]_2[Sn_2S_6] \cdot 2H_2O$ at 200K and room temperature (RT).

$[Ni(tren)(1,2\text{-}dap)]_2[Sn_2S_6] \cdot 2H_2O$	
200K	RT
a: 12.9264(3) Å	a: 13.0486(9) Å
b: 10.1627(3) Å	b: 10.1623(2) Å
c: 15.6585(4) Å	c: 15.7482(1) Å

Syntheses at room temperature (stirring conditions)

Table S3: Overview of the reaction conditions and resulting products of the syntheses at room temperature (t = 1-10 h). Total volume of the solvent 2 mL.

Ni educt 0.5 mmol	solvent	amount amine	product	yield
$\{[Ni(tren)]_2[Sn_2S_6]\}_n$ (**1**)$_n$	ma[a]	1.5 mL (17.2 mmol)	$[Ni(tren)(ma)(H_2O)]_2[Sn_2S_6]\cdot 4H_2O$ (**2**)	60%
	1,2dap	64 µL (0.75 mmol) – 2 mL (23.5 mmol)	$[Ni(tren)(1,2dap)]_2[Sn_2S_6]\cdot 2H_2O$ (**3**)	70%
	en	50 µL (0.75 mmol) – 2 mL (29.9 mmol)	$[Ni(en)_3]_2[Sn_2S_6]$[b]	70%
	1,2dach	90 µL (0.75 mmol) – 2 mL (16.6 mmol)	$[Ni(1,2dach)_3]_2[Sn_2S_6]\cdot 4H_2O$[c]	70%
	1,3dap	63 µL (0.75 mmol) – 2 mL (23.7 mmol)	$\{[Ni(tren)]_2[Sn_2S_6]\}_n$ (**1**)	90%

a: aqueous solution 40%

b: Behrens, M.; Scherb, S.; Näther, C.; Bensch, W. *Z. Anorg. Allg. Chem.* **2003**, *629*, 1367–1373.

c: Pienack, N.; Lühmann, H.; Seidlhofer, B.; Ammermann, J.; Zeisler, C.; Danker, F.; Näther, C.; Bensch, W. *Solid State Sci.* **2014**, *33*, 67–72.

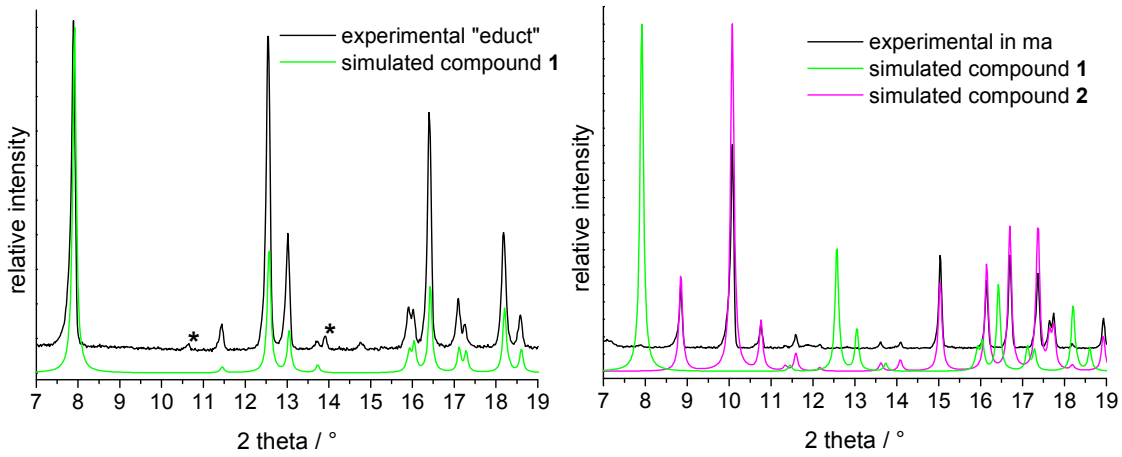

Fig. S2: PXRD pattern of compound **1** (left) which was then stirred with ma at room temperature resulting in formation of compound **2** (right). The by-product in compound **1** could not be identified (additional peaks are marked with an asterisk).

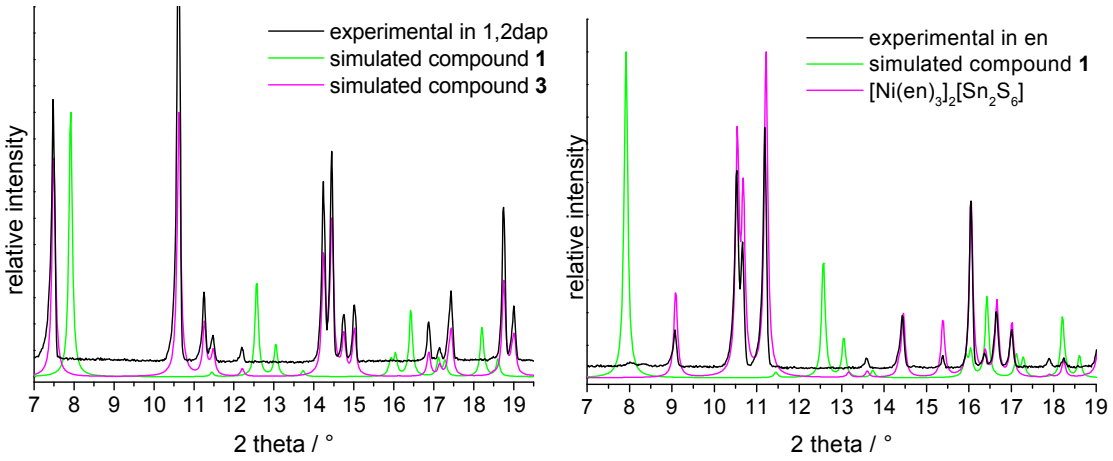

Fig. S3: PXRD pattern of the obtained products when stirring compound **1** at room temperature with 1,2-dap (resulting in **3**, left) and en (resulting in $[Ni(en)_2]_2[Sn_2S_6]$, right).

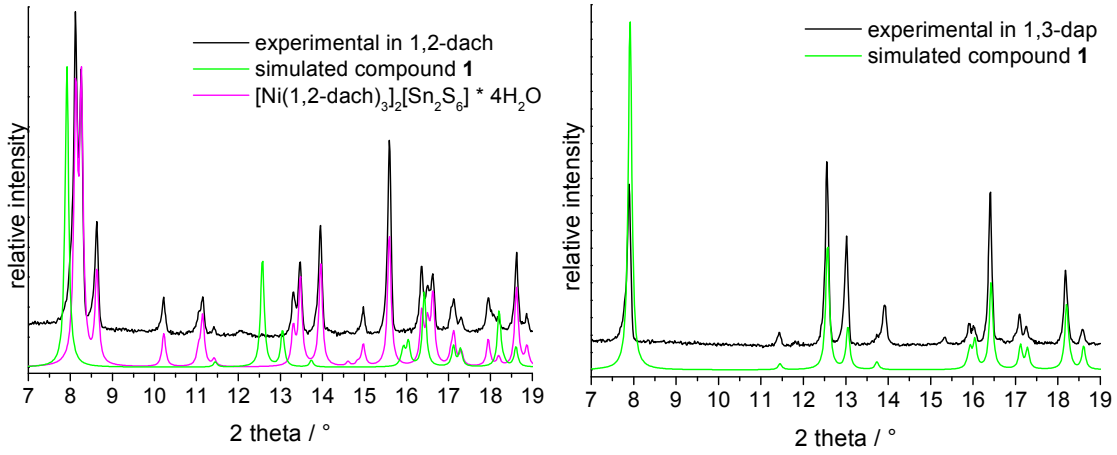

Fig. S4: PXRD pattern of the obtained results when stirring compound **1** at room temperature with 1,2-dach (resulting in $[Ni(1,2\text{-dach})_2]_2[Sn_2S_6] \cdot 4H_2O$, left) and 1,3-dap (regaining **1**, right).

Results obtained under stirring solvothermal conditions

Table S4: Overview of the resulting products under stirring conditions (T = 120°C; t = 1-10 h). Further educts: Sn (0.25 mmol) and S (0.75 mmol). Total volume of the solvent 2 mL.

Ni educts (0.25 mmol)	solvent	amount amine	product	yield
$\{[Ni(tren)]_2[Sn_2S_6]\}_n$ (**1**)	ma[a]	1.5 mL (17.2 mmol)	hot solution: $\{[Ni(tren)]_2[Sn_2S_6]\}_n$ (**1**)	90%
			RT: $[Ni(tren)(ma)(H_2O)]_2[Sn_2S_6]\cdot 4H_2O$ (**2**)	60%
	1,2dap	64 µL (0.75 mmol) – 2 mL (23.5 mmol)	$[Ni(tren)(1,2dap)]_2[Sn_2S_6] \cdot 2H_2O$ (**3**)	70%
	en	50 µL (0.75 mmol) – 2 mL (29.9 mmol)	$[Ni(en)_3]_2[Sn_2S_6]$[b]	70%
	1,2dach	90 µL (0.75 mmol) – 2 mL (16.6 mmol)	$[Ni(1,2dach)_3]_2[Sn_2S_6] \cdot 4H_2O$[c]	70%
	1,3dap	63 µL (0.75 mmol) – 2 mL (23.7 mmol)	$\{[Ni(tren)]_2[Sn_2S_6]\}_n$ (**1**)	90%

a: aqueous solution 40%

b: Behrens, M.; Scherb, S.; Näther, C.; Bensch, W. *Z. Anorg. Allg. Chem.* **2003**, *629*, 1367–1373.

c: Pienack, N.; Lühmann, H.; Seidlhofer, B.; Ammermann, J.; Zeisler, C.; Danker, F.; Näther, C.; Bensch, W. *Solid State Sci.* **2014**, *33*, 67–72.

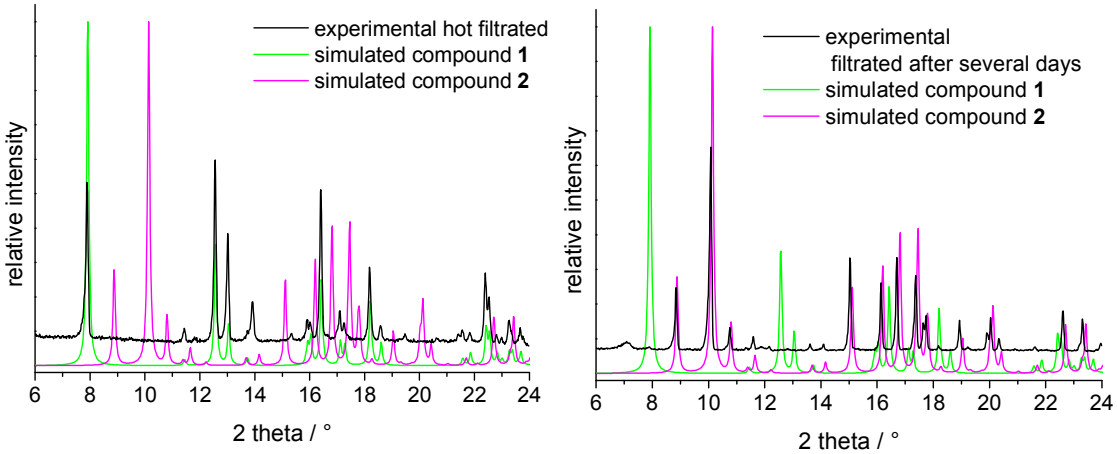

Fig. S5: PXRD pattern of the products obtained from the reaction mixture of **1** in ma (30%) when filtering the hot reaction mixture (left) and synthesis mixture after several days (right).

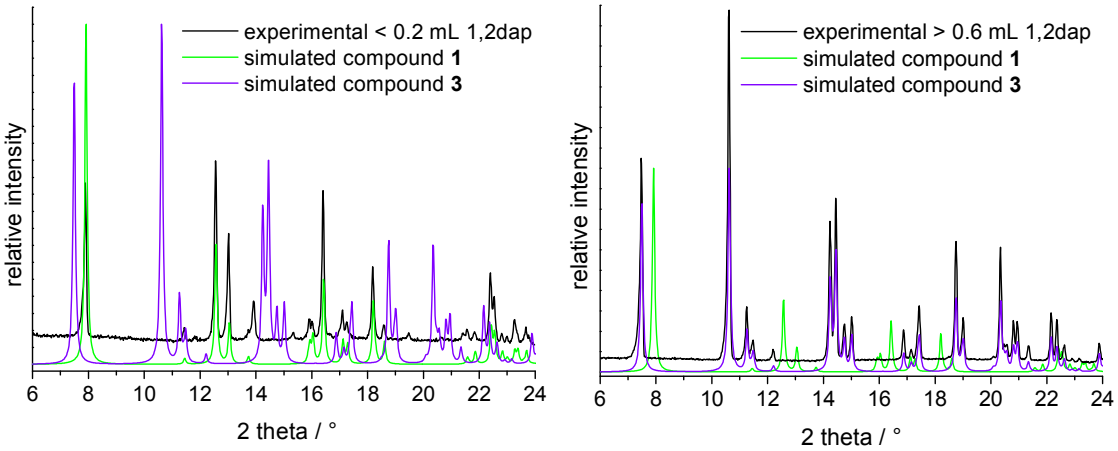

Fig. S6: PXRD pattern of the products obtained from the reaction mixture of **1** in an aqueous 1,2dap solution when applying < 0.2 mL (2.35 mmol) 1,2dap in the synthesis mixture (left) and > 0.6 mL 1,2dap (7.05 mmol) (RT) (right).

Spectroscopic Properties

Infrared spectroscopy

The observed absorptions in the IR spectra of compound **1**-**3** can be mostly assigned to tren [Marzotto, A; Ciccarese, A; Clemente, D. A.; Valle, G. *J. Chem. Soc. Dalton Trans.* **1995**, 1461-1468.] and the Ni-N-stretching vibration at below 420 cm^{-1}. The absorption of the other amines are mostly overlapping with the tren signals, but for example the absorption at 1206 and 828 cm^{-1} can be associate to a CH_3-group which is only present in compound **3** (Table S5).

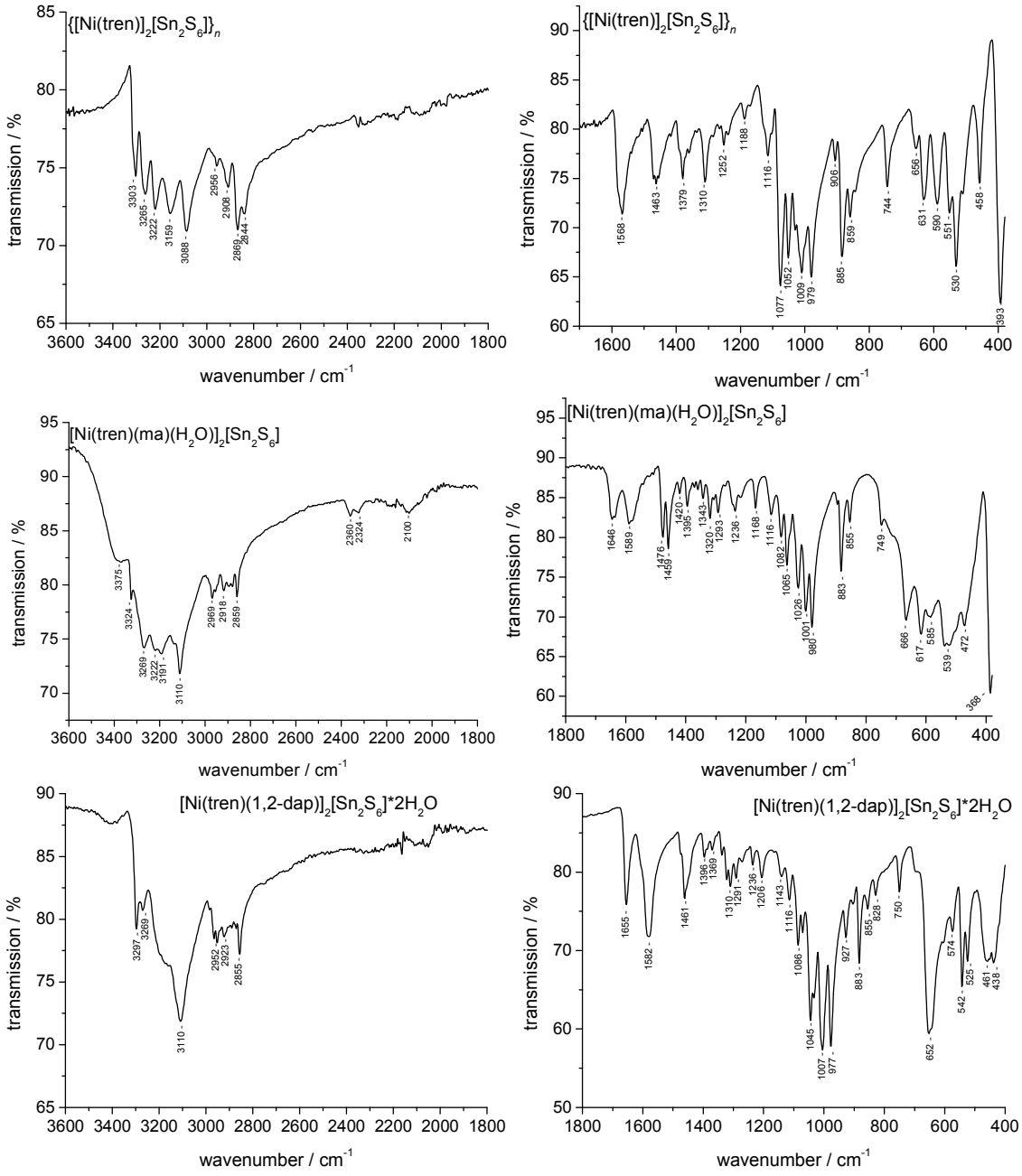

Fig. S7: IR spectra of **1-3**.

Table S5: Absorption of the IR spectra of compounds **1-3** compared to tris(2-aminethyl)amine (tren).

tren[Marzotto et al.]	**1**	**2**	**3**	assignment
		~3375	~3409	ν (O-H)
3270s	3303m, 3265m	3324m, 3269m	3297m, 3269w	ν (NH_2)
3180m	3222m, 3159m	3222w, 3191w, 3110s	3110s	ν (NH)
	3088m			ν (NH_2)
2930s, 2855s, 2800s	2956vw, 2908w, 2869m, 2844w	2969m, 2918w, 2859m	2966w, 2952w, 2923w, 2855m	ν (CH_2)
		2360w, 2324w, 2100w		ν (NH)
		1646m	1655m	δ(HOH)
1590s, 1445m	1568s, 1463m	1589m, 1476m, 1459m	1582s, 1461m	δ (NH_2) + ? (CH_2)
1390w, 1365(sh)	1379m	1420w, 1395w, 1361w	1396w, 1369w	δ (CH_2)
		1343w		δ (NH_2)
1348m, 1304m	1310m	1320w	1338w, 1323w, 1310w	δ (CH_2)
1270m, 1230w	1252w	1293w, 1236w	1291w, 1271vw, 1236w	ν (C-NH_2)+ ν (C-N)
			1206m	δ (CH_3)
	1188w	1168w	1143w	ν (C-N)
1112vs	1116m	1116w	1116m	ν (C-NH_2)+ ν (C-N)
1090m, 1070m, 1035s, 1020(sh)	1077s, 1052s, 1009s	1082w, 1065m, 1026m, 1001s	1086m, 1070w, 1045s, 1007s	δ (NH_2) region
	979s	980s	977s	
				skeleton vib. (cyclohex.)
902s (br), 865s(br), 840(sh)	906w, 885s, 859m	883s, 855m	927m, 906vw, 883m, 855w	δ (NH_2)
			828w	δ (CH_3)
765(sh), 730w	744m, 656w	749w, 666m	750m, 652s	δ (NH_2)
	631m, 590m, 551w, 530s, 458m	617m, 585w, 539m, 522m, 472w	574w, 542s, 525m, 461w,	main skeleton vib. (tren chain)
			438w	
	393s	386s		ν (M-N_{tren})

Raman spectroscopy

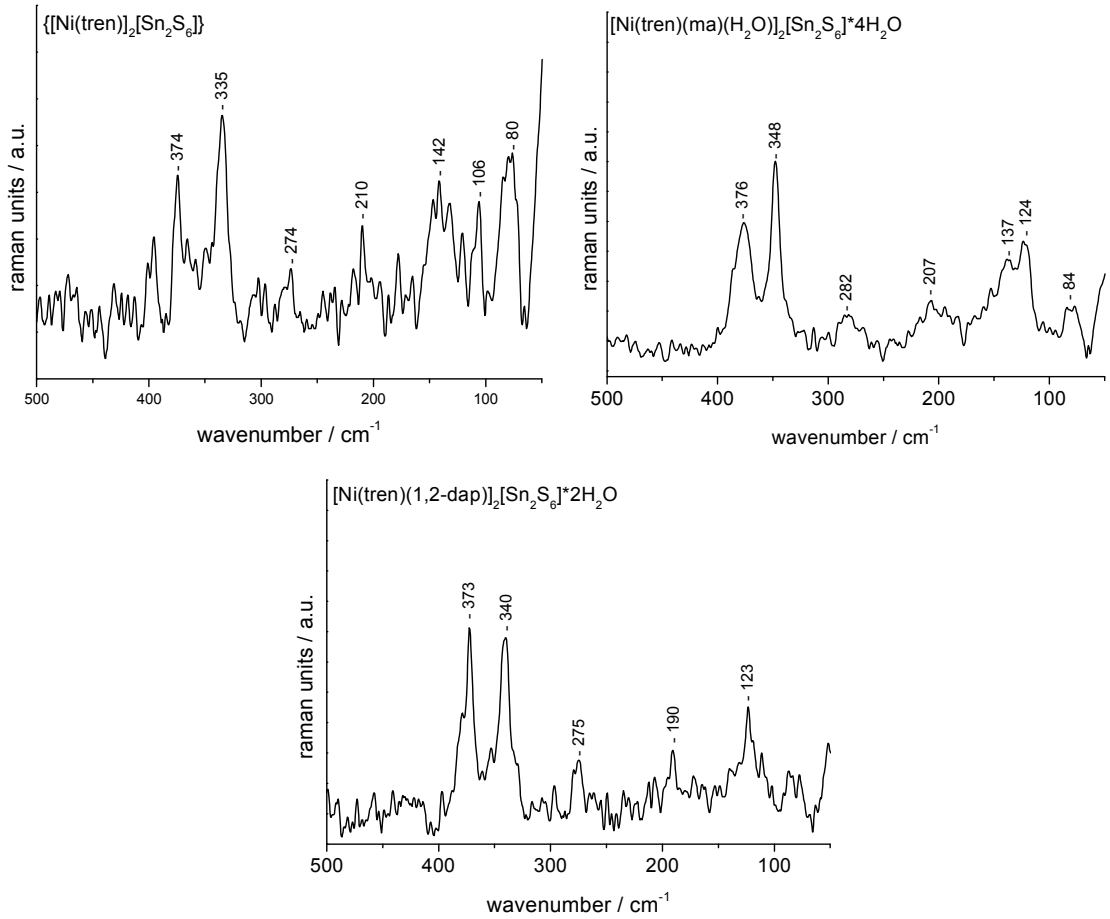

Fig. S8: Raman spectra of **1**-**3**.

Table S6: Data of the signals in the Raman spectra of $Na_4Sn_2S_6 \cdot 14\ H_2O$ [Krebs, B; Pohl, S.; Schiwy, W. *Angew. Chem. Int. Ed. Engl.* **1970**, *9*, 897-898] and compounds **1**-**3** (all wave numbers given in cm^{-1}).

$[Sn_2S_6]^{4-}$	**1**	**2**	**3**
391, 377	374	376	379, 373
341	335	348	340
281	274	282	275
190	210	207	190
151	178		
136	142	137	123
	106	124	
	80	84	

UV/vis spectroscopy

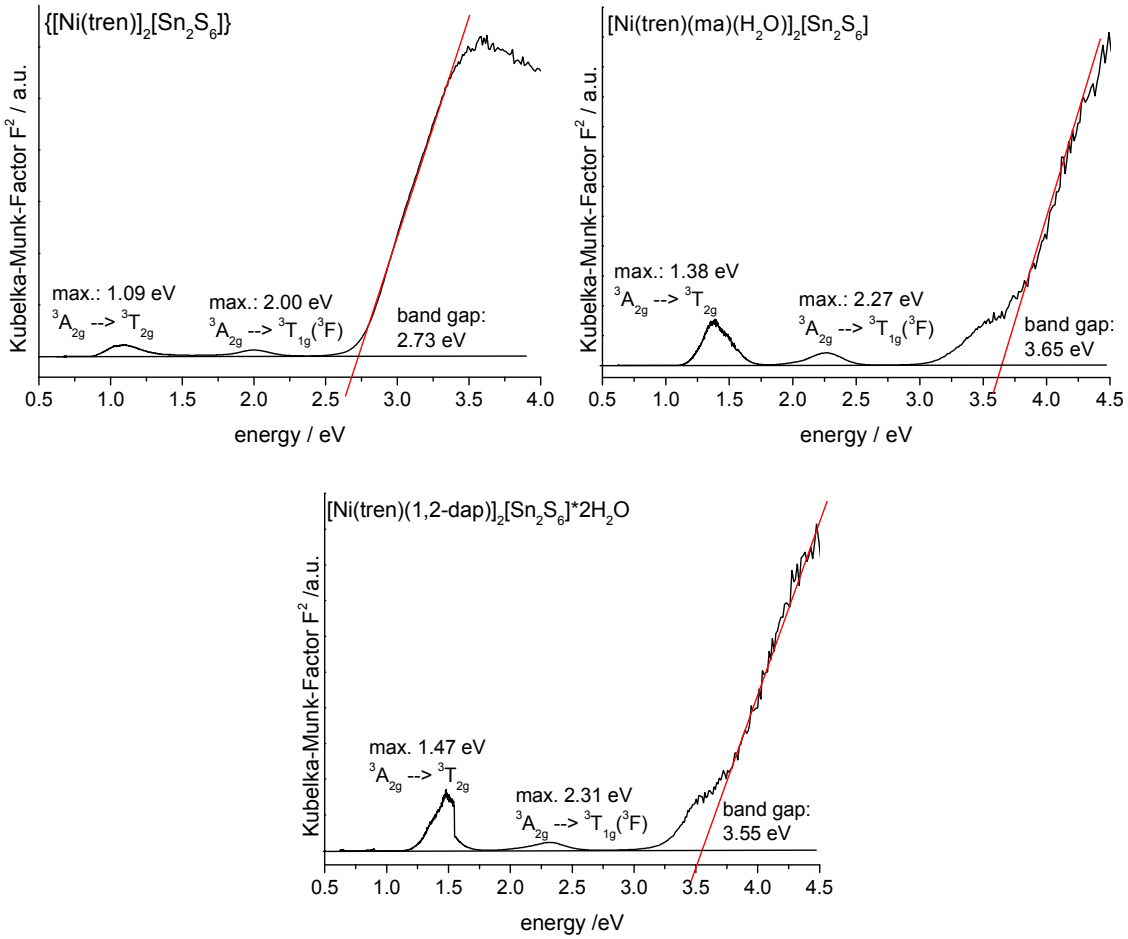

Fig. S9: Determination of the optical band gap of **1-3** from UV/vis diffuse reflectance spectrum using the Kubelka-Munk method.

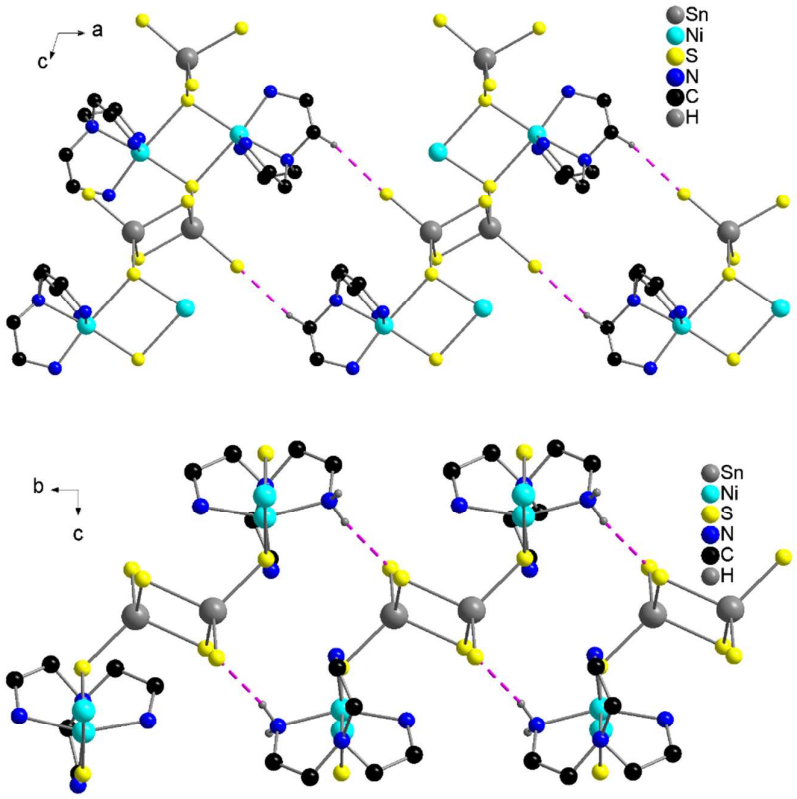

Fig. S10: Parallel arrangement of the $\{[Ni(tren)]_2[Sn_2S_6]\}_n$- chains within the *ac* plane (top) and bc-plane (bottom stabilized via hydrogen bridges (purple dashed lines).

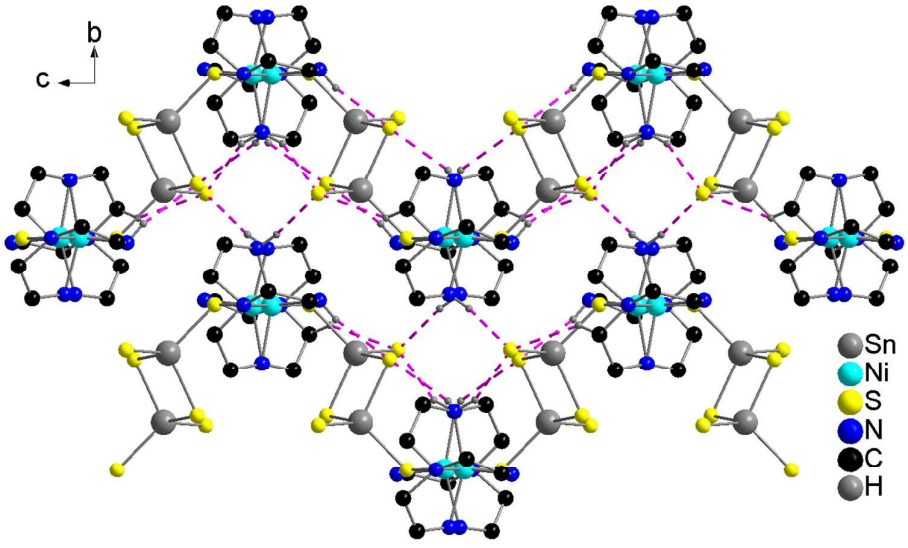

Fig. S11: Stabilizing of the structure in **1** via hydrogen bridges (purple dashed lines) within and between the chains.

Table S7: Calculated atomic distances (d/Å)

	Ni-N1	Ni-N2	Ni-N3	Ni-N4	Ni-S1	Ni-S2	N-H	S-Hc	Sn-S	Sn-S
XRD (exp)	2.088	2.102	2.115	2.130	2.434	2.745	1.036	-	2.311 2.363	2.452 2.467
Basis 1										
LDA	2.011	2.011	2.015	2.057	2.456	2.507	1.029 1.044		2.346 2.418	2.490 2.526
PBE	2.056	2.057	2.062	2.118	2.439	2.624	1.023 1.035		2.358 2.419	2.510 2.526
PBE0	2.055	2.056	2.058	2.100	2.462	2.694	1.011 1.020		2.333 2.385	2.478 2.490
Basis 2										
LDA	2.036	2.037	2.047	2.089	2.386	2.659	1.027 1.040		2.346 2.405	2.489 2.524
PBE	2.098	2.099	2.102	2.155	2.461	2.767	1.022 1.033		2.359 2.410	2.510 2.526
PBE0	2.095	2.104	2.104	2.140	2.481	2.825	1.013 1.023		2.334 2.381	2.478 2.490
Model 1										
LDA-BS1	2.035	2.035	2.045	2.045	2.373	2.374	1.031	1.366		
PBE-BS1	2.086	2.086	2.099	2.099	2.513	2.513	1.030	1.362		
B3LYP-BS1	2.072	2.072	2.089	2.089	2.452	2.452	1.018	1.346		
LDA-BS2	2.060	2.060	2.060	2.070	2.418	2.20	1.030	1.366		
PBE-BS2	2.125	2.125	2.125	2.135	2.590	2.591	1.027	1.362		
B3LYP-BS2	2.131	2.131	2.131	2.140	2.714	2.724	1.020	1.035		
Modell 2	BS1									
LDA-f	2.007	2.007	2.011	2.013	2.426	2.437	1.028	1.365		
LDA-BS1-af	2.008	2.008	2.020	2.011	2.407	2.424	1.029	1.373		
PBE-BS1-f	2.065	2.065	2.076	2.079	2.500	2.519	1.026	1.361		
PBE-BS1-af	2.069	2.069	2.069	2.077	2.493	2.495	1.026	1.365		
B3LYP-f	2.084	2.084	2.091	2.096	2.543	2.578	1.018	1.349		
B3LYP-af	2.086	2.092	2.095	2.095	2.544	2.551	1.018	1.350		
Mod2-BS2										
LDA-fm	2.031	2.031	2.037	2.040	2.464	2.476	1.028	1.365		
LDA-afm	2.034	2.034	2.036	2.036	2.443	2.464	1.028	1.372		
PBE-fm	2.101	2.101	2.116	2.120	2.540	2.567	1.026	1.361		
PBE-afm	2.103	2.103	2.115	2.118	2.537	2.545	1.025	1.365		
B3LYP-fm										
B3LYP-afm	2.126	2.126	2.134	2.140	2.584	2.617	1.018	1.351		

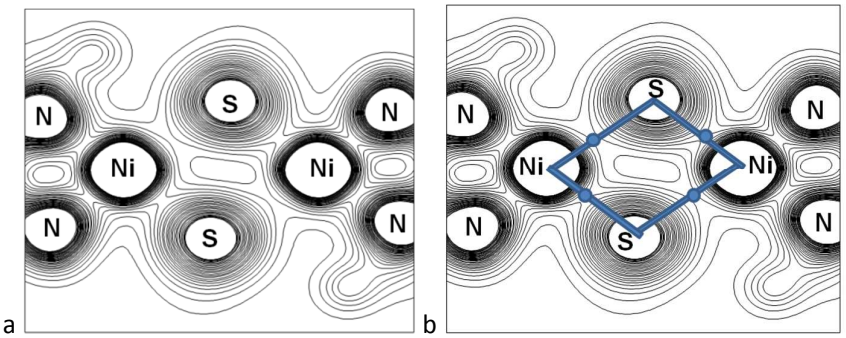

Fig. S12: a) Charge density plot for density values from 0.01 to 0.3 e/au³. The charge density at the BCP of the longer Ni-S bond is lower (0.029 e/au³) than for the shorter (0.051 e/au³, see also Tab. S8).

Table S8: BCP data for A-X bonds from the topological analysis of the charge density (PBE calculation) with calculated values at the BCPs for the charge density (ρ), its gradient, and its laplacian. ELF (Becke´s electron localisation function) values are calculated from α- (ELF) and ß-spin (ELFB) densities, and distances of the atoms to the BCP are given in Å.

BCP	Bond	ρ(e/au³)	Δρ	Δ²ρ	ELFA	ELFB	d(A-BCP)	d(BCP-X)
CP34	Sn-S	8.6625E-02	0	1.1815E-01	0.400	0.402	1.139	1.220
CP35	Sn-S	8.0602E-02	0	1.0433E-01	0.400	0.415	1.156	1.254
CP36	Sn-S	6.7958E-02	0	9.6166E-02	0.369	0.369	1.186	1.324
CP38	Sn-S	6.6023E-02	0	9.2107E-02	0.369	0.372	1.193	1.333
CP40	Ni-N	7.2764E-02	0	2.9572E-01	0.122	0.215	1.003	1.096
CP41	Ni-N	7.2711E-02	0	2.9330E-01	0.116	0.243	0.999	1.100
CP42	Ni-N	7.2313E-02	0	2.9049E-01	0.122	0.219	1.005	1.098
CP43	Ni-N	6.6176E-02	0	2.4589E-01	0.119	0.241	1.023	1.132
CP44	Ni-S	5.0957E-02	0	1.3404E-01	0.154	0.264	1.093	1.368
CP46	Ni-S	2.8845E-02	0	5.5496E-02	0.137	0.195	1.221	1.546
CP45	S-H	1.1371E-02	0	2.3027E-02	0.073	0.068	0.948	1.804
CP47	S-H	1.1647E-02	0	3.3221E-02	0.050	0.045	1.037	1.733
CP48	S-H	1.9349E-02	0	3.1873E-02	0.145	0.145	0.844	1.656
CP49	S-H	1.9205E-02	0	2.9482E-02	0.152	0.152	0.840	1.665
CP50	S-H	1.3211E-02	0	2.9092E-02	0.074	0.074	0.984	1.745
CP51	S-H	9.4996E-03	0	2.6443E-02	0.039	0.039	1.068	1.732

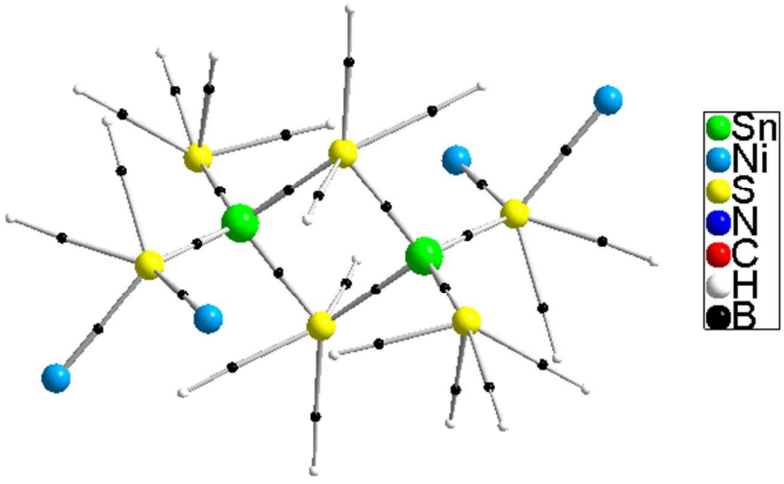

Fig. S13: Molgraph with all bonds and H-bonds at S atoms

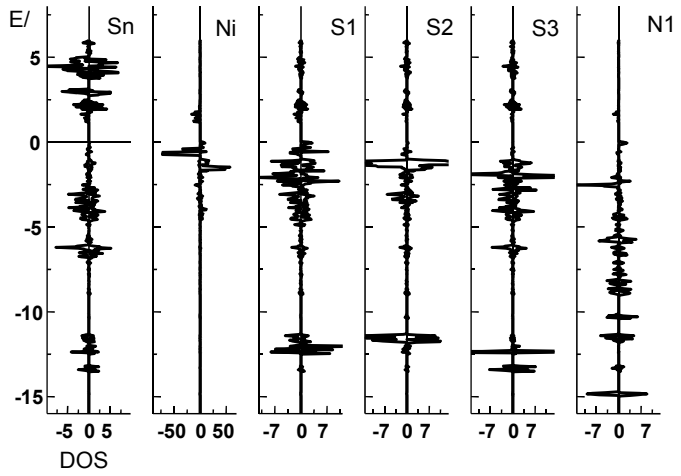

Fig. S14: Atomic site projected density of states (DOS) of the electronic band structure from the spin polarized PBE-calculation.

Octahedral coordination of the Ni^{2+} atom in compound **1**-**3** (Fig. S15, S16 and Table S9).

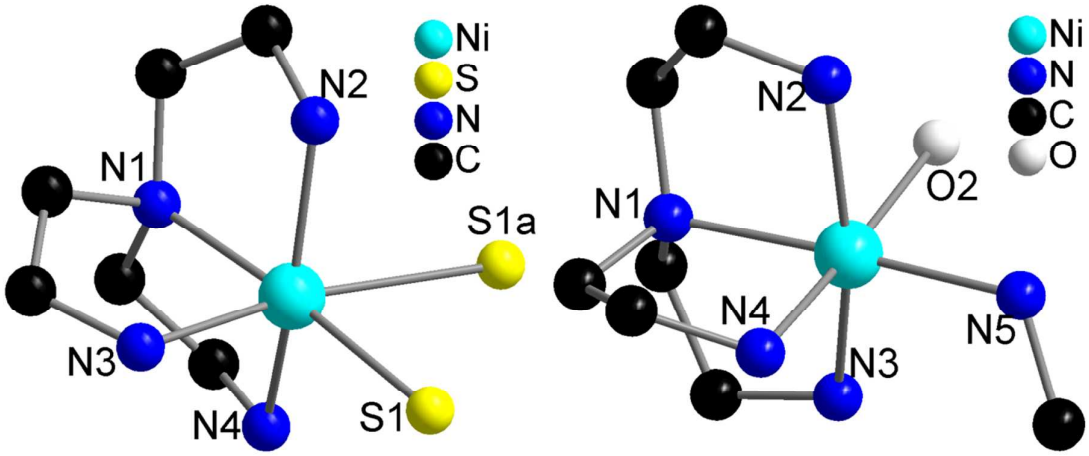

Fig .S15: Octahedral environment of the Ni^{2+} ion in compound **1** (top, left) and **2** (top, right).

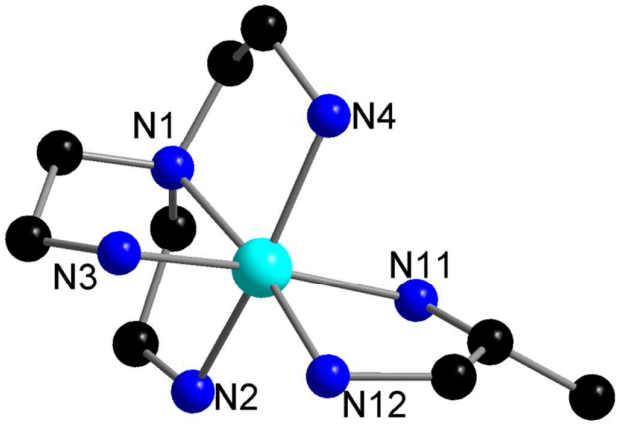

Fig. S16: Octahedral environment of the Ni^{2+} ion in compound **3**.

Table S9: Selected bond length (Å) and angles (°) of compounds **1** – **3** compared to $Na_4Sn_2S_6 \cdot 14H_2O$

	1[a]	**2**[b]	**3**[c]	$[Sn_2S_6]^{4-}$
Sn1 – S1	2.3634(3)	2.3412(7)	2.3343(7)	2.325
Sn1 – S2	2.3106(4)	2.3551(7)	2.3380(6)	2.338
Sn1 – S3	2.4523(3)	2.4433(6)	2.4512(6)	2.452
Sn1 – S3^x	2.4670(4)	2.4434(7)	2.4553(6)	2.448
S1 – Sn – S2	114.75(5)	120.61(3)	114.08(2)	119.8
S1 – Sn – S3	113.75(5)	111.11(3)	110.60(3)	108.2
S1 – Sn – S3^x	110.97(5)	110.37(2)	110.31(2)	110.4
S2 – Sn – S3	110.52(5)	108.11(2)	110.72(2)	110.6
S2 – Sn – S3^x	111.84(5)	109.45(2)	117.16(2)	110.8
S3 – Sn – S3^x	93.07(4)	93.92(2)	91.81(2)	94.0
Sn1 – S3 – Sn2/Sn1^x	86.93(4)	86.08(2)	88.18(5)	86.0
Ni1 – S1 – Ni2	80.98(5)	---	---	
S1 – Ni1 – S1^x	99.00(5)	---	---	
Ni1 – N1	2.130(4)	2.097(2)	2.120(4)	
Ni1 – N2	2.089(4)	2.138(2)	2.129(2)	
Ni1 – N3	2.102(5)	2.118(2)	2.115(2)	
Ni1 – N4	2.115(4)	2.090(2)	2.134(2)	
Ni1 – N5[2]/ N11[3]	---	2.089(2)	2.167(2)	
Ni1 – N12	---	---	2.091(2)	
Ni1 – S1	2.4343(4)	---	---	
Ni1 – S1^x	2.7449(5)	---	---	

Symmetry transformations used to generate equivalent atoms: x = a, b, c,
a: -x, y, ½-z; b: -x+2,-y+1,-z; c: -x,-y+1,-z+1

Table S10: Selected angles (°) of the octahedral Ni^{2+} environment of **1** and **2**.

1		**2**		**3**	
N(1)-Ni(1)-S(1)	174.27(13)	N(5)-Ni(1)-N(1)	174.82(9)	N(12)-Ni(1)-N(1)	171.43(9)
N(3)-Ni(1)-S(1)a	171.36(13)	N(4)-Ni(1)-O(2)	177.48(8)	N(3)-Ni(1)-N(11)	171.68(8)
N(2)-Ni(2)-N(4)	154.48(17)	N(3)-Ni(1)-N(2)	161.64(9)	N(2)-Ni(1)-N(4)	160.93(8)
N(3)-Ni(2)-S(1)	92.52(13)	N(5)-Ni(1)-N(4)	90.97(9)	N(12)-Ni(1)-N(3)	90.58(9)
N(3)-Ni(2)-N(1)	81.81(18)	N(4)-Ni(1)-N(1)	83.98(9)	N(3)-Ni(1)-N(1)	82.31(8)
N(4)-Ni(2)-S(1)	98.30(13)	N(5)-Ni(1)-N(3)	98.95(10)	N(12)-Ni(1)-N(2)	94.73(9)
N(4)-Ni(2)-N(1)	81.52(17)	N(1)-Ni(1)-N(3)	82.74(9)	N(1)-Ni(1)-N(2)	80.91(8)
N(3)- Ni(2)-N(4)	95.69(18)	N(4)-Ni(1)-N(3)	95.29(9)	N(3)-Ni(1)-N(2)	92.78(8)
S(1)-Ni(1)-S(1)a	80.98(5)	N(5)-Ni(1)-O(2)	90.34(9)	N(12)-Ni(1)-N(11)	81.11(8)
N(1)-Ni(1)-S(1)a	104.57(13)	N(1)-Ni(1)-O(2)	94.65(8)	N(1)-Ni(1)-N(11)	105.94(7)
N(4)-Ni(1)-S(1)a	79.75 (13)	N(3)-Ni(1)-O(2)	86.63(8)	N(2)-Ni(1)-N(11)	87.55(8)
N(2)-Ni(1)-S(1)	101.74(13)	N(5)-Ni(1)-N(2)	96.52(10)	N(12)-Ni(1)-N(4)	102.62(10)
N(2)-Ni(1)-N(1)	80.10(17)	N(1)-Ni(1)-N(2)	82.72(9)	N(1)-Ni(1)-N(4)	82.84(8)
N(2)-Ni(1)-S(1)a	87.91(13)	N(2)-Ni(1)-O(2)	86.63(8)	N(4)-Ni(1)-N(11)	87.38(8)
N(2)-Ni(1)-N(3)	99.04(18)	N(4)-Ni(1)-N(2)	94.26(9)		

Symmetry transformations used to generate equivalent atoms: a: -x, y, ½-z

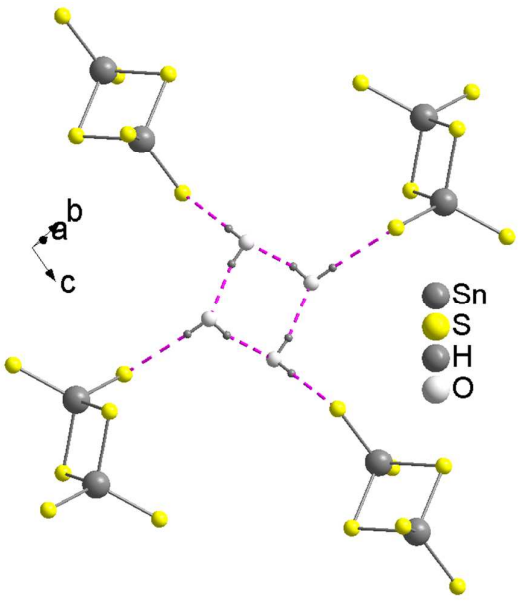

Fig. S17: Hydrogen bridging interactions of the water molecules in **2** with each other and with adjacent $[Sn_2S_6]^{4-}$ units.

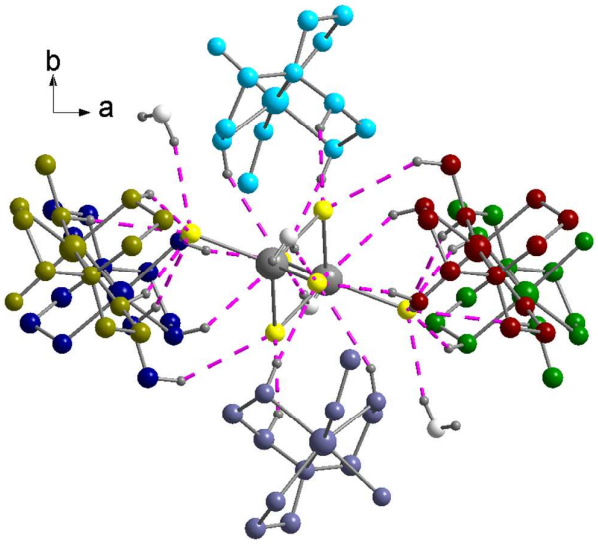

Fig. S18: Maximum hydrogen bridging interactions of the $[Sn_2S_6]^{4-}$ unit with adjacent molecules in **2**, only selected hydrogen atoms are shown.

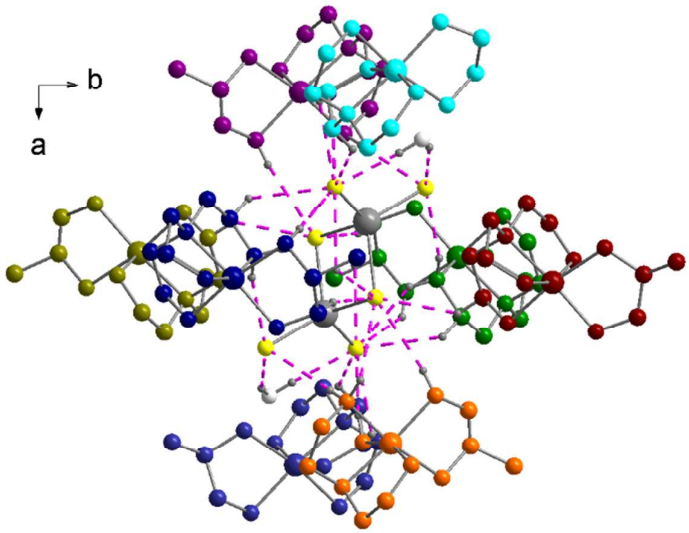

Fig. S19: Maximum hydrogen bridging interactions of the $[Sn_2S_6]^{4-}$ unit with adjacent molecules in **3**, only selected hydrogen atoms are depicted.